A non-newtonian model of blood capturing segregation of erythrocytes

Marek Čapek

Charles University in Prague, Faculty of Mathematics and Physics,
Mathematical Institute, Sokolovská 83, 186 75 Prague, Czech Republic

April 1, 2014

Abstract

In this paper we introduce key rheological properties of blood which are essential for blood coagulation process modelling. The conditions of blood flow determine the blood coagulation process, because blood flow carries chemical reactants to the area of the coagulation. Blood species are also expelled toward the vessel walls because there is inward migration of erythrocytes. We present a review of possible approaches to the blood flow modelling and formulate model of blood which contains hematocrit as an advected field. The inclusion enables model appropriately the expulsion of the other blood species towards vessel walls. We use in our cased microstructure based model of Owens[8]. We present an modification of Owens' model, which couples new information from the hematocrit field. The segregation of erythrocytes is treated under simplyfying assumption on erythrocytes, which enable to use the framework of suspension rheology[21],[22]. The governing equations are solved for some simplified computational domains.

1 Introduction

1.1 Motivation for studying blood flow

Blood coagulation is a phenomenon whose physiological function is to prevent blood losses due to injury to vessel wall. Blood coagulation can also occur because of some pathological diseases such as arteriosclerosis, one of the lifestyle diseases. In such situations the coagulation is initiated without vessel wall injury. Blood coagulation can also occur on the surface of medical devices, which can be very unwelcome. Thus better understanding of the coagulation process could help us to improve the quality and length of contemporary human life.

1.2 Blood properties

Whole blood consists mainly of plasma, red blood cells (RBCs) or erythrocytes, white blood cells or leukocytes and platelets or thrombocytes. Over one half of the volume of total blood consists of plasma, RBCs make up 40-45% volume of blood; this value is called haematocrit. Blood plasma behaves as Newtonian fluid with low apparent viscosity. In the following we will use terms viscosity and apparent viscosity interchangeably. Under normal conditions in the circulatory system RBCs determine the properties of the whole blood. They are 6-8μm in diameter and 2μm thick discoid shaped cells, which have an elastic membrane on the surface and which are filled with haemoglobin. These features enable them to change shape easily. RBCs form under low shear rate flow conditions column-like structures called rouleaux, which cause an increase in viscosity. These structures break up as shear rate increases. As RBCs have very strong influence on the whole blood, the viscosity of blood has shear-thinning character. Due to the elasticity of RBCs, blood stores mechanical energy, which leads to viscoelastic

behaviour of the whole blood, as Thurston [1] firstly recognized. Therefore blood behaves as viscoelastic fluid in small veins, where RBC deforms and stores elastic energy, while in larger arteries blood can be taken as Newtonian fluid with shear-thinning viscosity. It is known from experiments (see [2]) that red blood cells stack around the middle of the vessel. They push the platelets away from the centre of the vessel. Platelets are then concentrated mainly at the walls.
Blood coagulation begins under vessel injury conditions by the activation of blood platelets. This is caused by exposition of specific chemicals in the endothelium of the vessel wall. Blood platelets can also be activated by a prolonged exposure to a high or rapid increase in shear stress that leads to erythrocytes and platelets damage (see [3]). The exposition of the chemical in the endothelium triggers the so called coagulation cascade , which is a complex set of enzymatic reactions with both positive and negative feedbacks (see [4]). General structure of each reaction is conversion of pro enzyme, zymogen, which is non-active precursor of enzyme, to active enzyme. This activated enzyme then enables subsequent reactions proenzyme-enzyme in the cascade. The whole complex of reactions ends with the transformation of fibrinogen to fibrin. Fibrin strands then link together with the activated platelets in order to form the final cross-linked fibrin clot.

1.3 An challenge for blood rheology

Most blood coagulation models have concentrated either on biochemistry of the process or rheology of blood flow. Combination of the two aproaches is necessary in order to realistically describe blood coagulation process.
Erythrocytes tend to push out blood platelets towards vessel walls, as was said above. We have to add that other blood species such as white blood cells and the chemical species taking part in the blood coagulation process are expelled towards vessel walls too.
This feature of blood flow is very important as platelets and the chemical species participating in the blood coagulation process are close to the area of vessel wall injury.
Therefore we will try to develop a model fo blood flow, which will capture the migration of platelets towards vessel walls. It seems reasonable to add to the constitutive equations for blood an advected field representing the volume fraction of red blood cells - hematocrit. The local number of erythrocytes will then give us the information about the presence of other blood species, e.g. blood platelets.
We will advocate an microstructure based model of blood of Owens [8], because it seems to us, that such a kind of model is most appropriate for the proposed aim of realistic blood coagulation process modelling.

1.4 Mathematical modelling

There is large number of mathematical models of blood flow. They can be categorized according several criteria. We will use the criterion of the size of the vessel, blood is flowing in. We divide vessels into large vessels, 'medium' vessels and vessels which are part of so called microcrocirculation. We define large vessel as veins or arteries of the size from 1 to 3cm. Smaller vessels which we call 'medium' vessels have size from 0.2mm to 1 cm. We take even smaller vessels as a part of microcirculation system.
Such a division seems to be reasonable from rheological point of view. From experiment we know that blood exhibits shear-thinning behaviour. In large vessels, where high values of shear rate are present, we are in the area of constant viscosity. It is therefore adequate to treat blood in this case as Newtonian fluid with constant viscosity. In this case we finally end with Navier-Stokes equations with constant viscosity. What is more in the large vessels the viscoelastic properties of blood are not so prominent as in small- and medium- sized vessels.
The vessels which are part of microcirculation system are also characteristic by the fact, that size of red blood cells in the vessel is comparable to the size of the vessel. The blood flow in these vessels can not described by continuum mechanics approach, it is necessary to trace the red blood cells individually.
The vessels of 'medium' size are most interesting for us. The blood in these vessels exhibits shear-thinning properties and viscoelasticity.
However it must be said, that shear-thinning properties and viscoelasticity of blood is also apparent under pathological conditions in large vessels, e.g. aneurytic or stenotic vessel.

2 Mathematical modelling in 'medium' sized vessels

The viscoelastic features of the blood are most visible in 'medium' sized vessels. In these vessel is still reasonable the approach of continuum mechanics modelling as red blood cells are much more smaller than the vessel they are flowing in.
However to be precise it is still possible to model blood flow with particle-based approach, as could be seen from the following paragraph

Lattice-Boltzmann methods for blood flow [16] developed a model of blood based on the Immersed Boundary method. Blood is modelled as composite of viscous fluid and objects suspended in it - red blood cells. It is supposed that both plasma and aquaeus solution in red blood cells behave like Newtonian fluids. It is used the Eulerian description for the viscous fluid and the Lagrangian description for the suspended particles.
This type of modelling could seem to be attractive as it provides very precise results. However it is very computationally demanding and as it is said in [16] even 2D simulations are very expensive, not to mention 3D computations. The preciseness of this approach can be also discussed from another point of view - do we really need to know the positions of each red blood cell during the simulation if we are already in a medium sized vessel.

We will go on categorizing possible models of blood flow by dividing the models into two groups

- phenomenological
- microstructure based

It is interesting to note, that sometimes we can arrive at the same model with phenomenological or microstructure based model, e.g. Oldroyd-B model.

2.1 Phenomenologically based models

We divide phenomenological models into two categories.
Phenomenological models of the first type are models derived by supposition of quite general forms of constitutive equations, i.e. stress tensor. Generality of these forms is then restricted by application of reasonable constraints, for instance principle of material frame indifference. We will call this type of phenomenological modelling traditional.
The second approach is based on the principle of maximization of rate of entropy production, i.e. a principle of extended non-equilibrium thermodynamics.

2.1.1 Traditional phenomenological modelling - the Generalized Newtonian Fluid

If we say that a fluid is Newtonian we mean, that following relation holds:

$$\mathbf{T} = 2\eta_0\mathbf{D}, \tag{2.1}$$

where $\mathbf{T}$ and $\mathbf{D}$ is extra stress tensor and deformation tensor, respectively. η_0 is constant viscosity.
To obtain more general constitutive equations, we abandon the linear dependence of extra stress tensor on deformation tensor expressed by previous equation. In order to derive a model independent of coordinate system we write viscosity as a function of principal invariants of $\mathbf{D}$. If we further suppose incompressibility of the fluid and simple shear flow configuration we get the viscosity dependence only on shear rate $\dot{\gamma}$ defined as

$$\dot{\gamma} = \sqrt{\frac{1}{2}\mathbf{D} : \mathbf{D}}. \tag{2.2}$$

Therefore we get

$$\mathbf{T} = 2\eta(\dot{\gamma})\mathbf{D}. \tag{2.3}$$

The most famous example of this type of constitutive modells is power-law model:

$$\mathbf{T} = 2|\dot{\gamma}|^{\frac{(n-1)}{2}}\mathbf{D}. \tag{2.4}$$

The generalized Newtonian fluid is a simple model. It describes accurately only such fluids, where elastic effects are negligible and the shear-thinning effect has a strong influence on the flow behaviour.
Some computations of blood flow using these simple models were carried out, see [12] and [13]. However these simulations do not take into account the elasticity of blood.
It is therefore necessary to arrive at viscoelastic model of blood.

2.1.2 Traditional phenomenological modelling - example Oldroyd-B derivation

A simple viscoelastic model can be derived using this procedure, see [23] for details. The procedure reads:

- writing equations for 1D mechanical analog
- switching to 2D, resp. 3D
- introduction of objective time derivative

The Oldroyd-B model, which will be derived in alternative way below, can be inferred by the procedure sketched here.

2.1.3 Modern phenomenological modelling- example Oldroyd-B derivation

In the following we will use the thermodynamical framework developed in [5],[6] and [7]. The crux of the procedure lies in choosing a specific form of thermodymical scalar quantity, i.e. the rate of entropy production. The rate is then maximised and constitutive equations can be derived.

Let $\kappa_R(B)$ and $\kappa_t(B)$ be the reference and the current configuration of the body B. $\kappa_{p(t)}(B)$ is stress-free configuration obtained by instantaneously unloading the body from its current configuration. The motion of the body is a one-to-one mapping between the reference

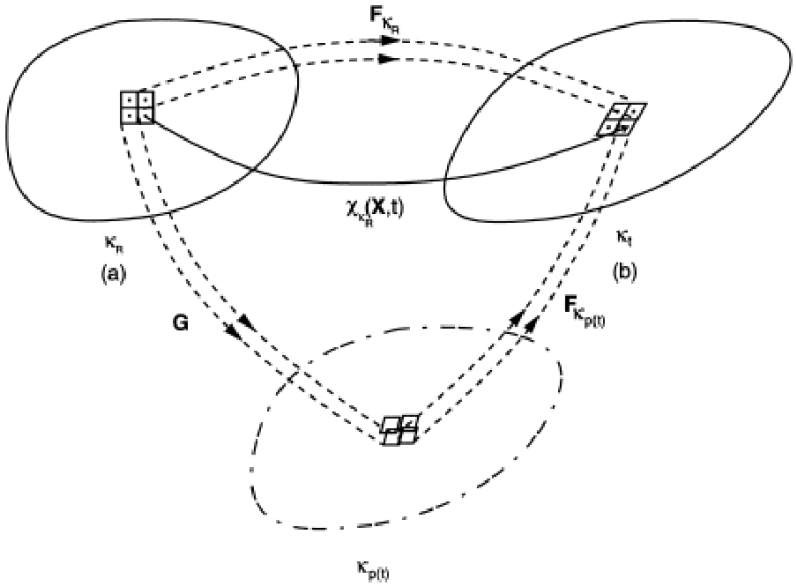

Figure 1: Natural configuration. From [5]

configuration and the current configuration, i.e.

$$\mathbf{x} = \chi_{\kappa_R}(\mathbf{X}, t). \tag{2.5}$$

We define the deformation gradient

$$\mathbf{F}_{\kappa_R} = \frac{\partial \chi_{\kappa_R}}{\partial \mathbf{X}_{\kappa_R}} \tag{2.6}$$

and left Cauchy-Green stretch tensor

$$\mathbf{B}_{\kappa_R} = \mathbf{F}_{\kappa_R}\mathbf{F}^T_{\kappa_R}. \tag{2.7}$$

The tensor $\mathbf{F}_{\kappa_{p(t)}}$ represents the mapping, deformation gradient, from an infinitesimal element of $\kappa_{p(t)}$ to κ_t. The left Cauchy-Greenn stretch tensor $\mathbf{B}_{\kappa_{p(t)}}$ is defined corespondingly.
Let us define the mapping from κ_R to $\kappa_{p(t)}$

$$\mathbf{G} = \mathbf{F}_{\kappa_R \to \kappa_{p(t)}} = \mathbf{F}^{-1}_{\kappa_{p(t)}}\mathbf{F}_{\kappa_R}. \tag{2.8}$$

We define velocity gradients $\mathbf{L}$ and $\mathbf{L}_{\kappa_{p(t)}}$ as

$$\mathbf{L} = \dot{\mathbf{F}}_{\kappa_R}\mathbf{F}^{-1}_{\kappa_R} \tag{2.9}$$

and

$$\mathbf{L}_{\kappa_{p(t)}} = \dot{\mathbf{G}}\mathbf{G}^{-1}. \tag{2.10}$$

The rate of dissipation ξ associated with the material is defined by

$$\xi = \mathbf{T}\cdot\mathbf{D} - \dot{W}. \tag{2.11}$$

The form of the rate of dissipation chosen for the derivation of Oldroyd-B like fluid is

$$\xi = \tilde{\xi}(\mathbf{D}, \mathbf{D}_{\kappa_{p(t)}}, \mathbf{B}_{\kappa_{p(t)}}) = 2\nu_0|\mathbf{D}|^2 + 2\nu_1\mathbf{D}_{\kappa_{p(t)}}\cdot\mathbf{B}_{\kappa_{p(t)}}\mathbf{D}_{\kappa_{p(t)}}. \tag{2.12}$$

We perform the procedure of maximization of entropy production (we have only a mechanical settings, i.e. the rate of dissipation equals the rate of entropy production) with following incompressibility constraints

$$tr(\mathbf{D}) = 0, \tag{2.13}$$

$$tr(\mathbf{D}_{\kappa_{p(t)}}) = 0. \tag{2.14}$$

We also suppose the following form of stored energy (neo-Hookean)

$$W = \frac{\mu}{2}(tr\mathbf{B} - 3). \tag{2.15}$$

After some calculation we arrive at the following system of equations of rate type nonlinear viscoelastic model

$$\begin{gathered} div\mathbf{v} = 0, \\ \rho\dot{\mathbf{v}} = div\mathbf{T}, \\ \mathbf{T} = -p\mathbf{I} + 2\nu_0\mathbf{D} + \mu\mathbf{B}^d_{\kappa_{p(t)}}, \\ 2\nu_1\left(-\frac{1}{2}\overset{\triangledown\, d}{\mathbf{B}}_{\kappa_{p(t)}} - \frac{1}{3}(\mathbf{D}\cdot\mathbf{B}^d_{\kappa_{p(t)}})\mathbf{I} + \frac{1}{3}(tr\mathbf{B}_{\kappa_{p(t)}})\mathbf{D}\right) = \mu\mathbf{B}^d_{\kappa_{p(t)}}, \\ det\left(\mathbf{B}_{\kappa_{p(t)}} + \frac{1}{3}(tr\mathbf{B}_{\kappa_{p(t)}})\mathbf{I}\right). \end{gathered} \tag{2.16}$$

It is possible to perform linearization, i.e. suppose that $\mathbf{B}_{\kappa_{p(t)}} = \mathbf{I} + \mathbf{A}$, where $\|A\| = \epsilon$, $0 < \epsilon << 1$. After substitution into the nonlinear model we neglect all elements of order ϵ^2 and higher. Having finished the procedure we arrive at following set of equations

$$\begin{gathered} div\mathbf{v} = 0, \\ \rho\dot{\mathbf{v}} = div\mathbf{T}, \\ \mathbf{T} = -p\mathbf{I} + 2\nu_0\mathbf{D} + \mu\mathbf{A}, \\ \mu\mathbf{A} + \nu_1\overset{\triangledown}{\mathbf{A}} = 2\nu_1\mathbf{D}. \end{gathered} \tag{2.17}$$

It can be seen, that we arrived at Oldroyd-B model via an alternative framework, which is thermodynamically consistent.

2.1.4 Modern phenomenological modelling-Anand's model of blood

Anand [14] developed a complex model for blood clotting process. One part of the model is blood continuum model, which is derived similarly as Oldroyd-B model.
The rate of dissipation chosen by Anand has following form:

$$\xi = \alpha^b \left(\mathbf{D}_{\kappa_p(t)} \cdot \mathbf{D}_{\kappa_p(t)}\mathbf{D}_{\kappa_p(t)}\right)^{\gamma^b} + \eta_1^b \mathbf{D} \cdot \mathbf{D}, \tag{2.18}$$

which correspond to a mixture of a viscoelastic fluid that has a power-law viscosity and a Newtonian-fluid. α^b is a shear-thinning viscosity, η_1^b is the viscosity of plasma,γ^b is a shear-thinning index. Anand takes neo-Hookean form of stored energy:

$$W = \frac{\mu^b}{2}(I_{\mathbf{B}} - 3), \tag{2.19}$$

where μ^b an elastic modulus. The final model for the blood continuum takes this form

$$\begin{aligned}
\mathbf{T} &= -p\mathbf{1} + \mathbf{S}, \\
\mathbf{S} &= \mu^b \mathbf{B}_{\kappa_p(t)}, + \eta_1^b \mathbf{D} \\
\overset{\triangledown}{\mathbf{B}}_{\kappa_p(t)} &= -2\left(\frac{\mu^b}{\alpha^b}\right)^{1+2n^b} \left(tr(\mathbf{B}_{\kappa_p(t)}) - 3\lambda\right)^{n^b} \left[\mathbf{B}_{\kappa_p(t)} - \lambda\mathbf{1}\right], \\
\lambda &= \frac{3}{tr(\mathbf{B}^{-1}_{\kappa_p(t)})}, \\
n^b &= \frac{\gamma^b - 1}{1 - 2\gamma^b}; n^b > 0.
\end{aligned} \tag{2.20}$$

Remark: Although the phenomenological models are developed in an elegant way, they seem to underestimate the role of aggregation and disaggregation of rouleaux leading to specific rheological behaviour of blood such as thixotropy. Indeed the Anand's model was fitted to experimental data in steady Poiseuille flow and oscillatory flow. Anand stated that the model can be fitted to experimenat results of Bureau, but it was now shown in the Anand's work.
One remedy for unability of a model to capture the microstructure related phenomena is to make the microstructure part of the model. As thixotropy is a phenomenon based on microstructure properties of blood it seems reasonable to add a field corresponding to the microstructure.
Recent development in the framework of Rajagopal has also shown, that the framework can also be used in such a way that fits well with data Bureau, see [15].
However it must be said, that the microstructure modelling has further advantages for us, which will be discussed later.

2.2 Microstructure based models

2.2.1 Example - derivation of Oldroyd-B

Above we arrived at Oldroyd-B model by two phenomenological approaches. In this part we derive Oldroyd-B by microstructure based modelling in order to show the relevance of this type of modelling. In the following sections we will derive microstructure based model of blood.
Microstructure based modelling has one great advantage over phenomenological modelling - the parameters that we discover in constitutive equations have clear physical interpretation. These parameters are namely related to the microstructure properties of fluid, which are measurable.
The Oldroyd-B model derivation is based on a simplification of basic microstructure in fluid flow - the elastic dumbbell model. The elastic dumbbell is an idealization consisting of two identical beads connected by a massless spring. The derivation of the constitutive model begins with postulation of the force balance

$$\mathbf{F_i^{(f)}} + \mathbf{F_i^{(c)}} + \mathbf{F_i^{(b)}} = 0 \qquad i = 1, 2, \tag{2.21}$$

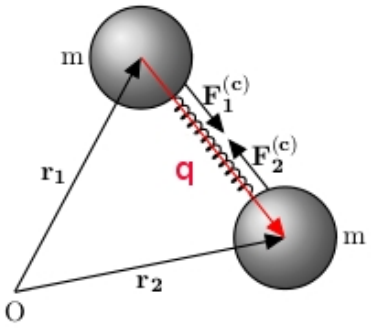

Figure 2: Elastic dumbbell

where $\mathbf{F_i^{(f)}}$ is a friction force, $\mathbf{F_i^{(c)}}$ a spring force, $\mathbf{F_i^{(b)}}$ a Brownian force. As we are dealing with the Brownian force, which is a stochastic process, we have to solve the following stochastic differential equastions for elements of $\mathbf{q}$ -the end to end vector of a dumbbell.

$$\frac{d\mathbf{q}}{dt} = \nabla\mathbf{u}\cdot\mathbf{q} - \frac{2H}{\zeta}\mathbf{q} - \sqrt{\frac{4kT}{\zeta}}d\mathbf{W}(t), \tag{2.22}$$

where ζ is so-called friction coefficient, $\boldsymbol{W}(t)$ is a multidimensional Wiener process, H is a spring constant, k is Boltzmann constant, T the temperature. A viable possibility how to solve the equation is to transform it to Fokker-Planck or diffusion equation

$$\frac{\partial}{\partial t}\psi(\mathbf{q},t) = -\frac{\partial}{\partial\mathbf{q}}\cdot\left[\left(\nabla\mathbf{u}\cdot\mathbf{q} - \frac{2H}{\zeta}\mathbf{q}\right)\psi(\mathbf{q},t) + \frac{2kT}{\zeta}\frac{\partial}{\partial\mathbf{q}}\psi(\mathbf{q},t)\right], \tag{2.23}$$

where $\psi(\mathbf{q},t)$ is the probability density function. Having the probability density function $\psi(\mathbf{q},t)$ we can define the expectation of $g(\mathbf{q})$ as

$$< g(\mathbf{q}) >= \int g(\mathbf{q})\psi(\mathbf{q},t)d\mathbf{q}. \tag{2.24}$$

From equation (2.23) we can derive the equation of change of $< g(\mathbf{q}) >$

$$\frac{d}{dt} < g(\mathbf{q}) >= \left\langle (\nabla\mathbf{u}\cdot\mathbf{q})\frac{\partial}{\partial\mathbf{q}}g(\mathbf{q})\right\rangle + \frac{2kT}{\zeta}\left\langle\frac{\partial}{\partial\mathbf{q}}\cdot\frac{\partial}{\partial\mathbf{q}}g(\mathbf{q})\right\rangle - \frac{2H}{\zeta}\left\langle\mathbf{q}\cdot\frac{\partial}{\partial\mathbf{q}}g(\mathbf{q})\right\rangle. \tag{2.25}$$

The equation for $g(\mathbf{q}) = \langle\mathbf{qq}\rangle$ takes the following form:

$$\frac{\partial}{\partial t}\langle\mathbf{qq}\rangle - \nabla\mathbf{u}\langle\mathbf{qq}\rangle - \langle\mathbf{qq}\rangle\nabla\mathbf{u}^T = \frac{4kT}{\zeta}\mathbf{I} - \frac{4H}{\zeta}\langle\mathbf{qq}\rangle. \tag{2.26}$$

Let us suppose the following decomposition of the total stress tensor $\boldsymbol{\sigma}$

$$\boldsymbol{\sigma} = \boldsymbol{\sigma}_S + \boldsymbol{\sigma}_P = (-p_S\mathbf{I} + \mathbf{T}_S) + (-p_P\mathbf{I} + \boldsymbol{\tau}) = -p\mathbf{I} + \mathbf{T}, \tag{2.27}$$

where $p = p_S + p_P$ and $T = \mathbf{T}_S + \boldsymbol{\tau} = 2\eta_S\mathbf{D} + \boldsymbol{\tau}$. Kramers performed elementary physical derivation of $\boldsymbol{\sigma}_P$. He got in the end so called Kramers expression for the extra-stress tensor

$$\mathbf{T} = \mathbf{T}_S + \boldsymbol{\tau} = 2\eta_S\mathbf{D} + nH < \mathbf{qq} > -nkT\mathbf{I}, \tag{2.28}$$

where n is the number density of dumbbells. On substitution of (2.26) in the previous equation we arrive at Giesekus expression

$$\mathbf{T} = 2\eta_S\mathbf{D} - \frac{n\zeta}{4} < \overset{\triangledown}{\mathbf{qq}} > . \tag{2.29}$$

We define the relaxation time

$$\lambda = \frac{\zeta}{4H}, \tag{2.30}$$

the polymeric viscosity

$$\eta_P = \frac{nkT\zeta}{4H} = nkT\lambda, \tag{2.31}$$

the total viscosity $\eta_0 = \eta_S + \eta_P$, the characteristic relaxation time

$$\lambda_r = \frac{\eta_S}{\eta_0}\lambda. \tag{2.32}$$

Then we can write the equation for the total extra stress tensor

$$\mathbf{T} + \lambda \overset{\triangledown}{\mathbf{T}} = 2\eta_0(\mathbf{D} + \lambda_r \overset{\triangledown}{\mathbf{D}}), \tag{2.33}$$

which is the Oldroyd-B model. We can write it int the form of split form of the Oldroyd-B model

$$\mathbf{T} = 2\eta_S\mathbf{D} + \boldsymbol{\tau}, \tag{2.34}$$

$$\boldsymbol{\tau} + \lambda \overset{\triangledown}{\boldsymbol{\tau}} = 2\eta_P\mathbf{D}. \tag{2.35}$$

2.2.2 Owens' model of blood

In Owens' model, see [8], [9] and [10] for details, a rouleaux containing k red blood cells is represented by an elastic dumbbell. Let $\psi_k(\mathbf{x}, \mathbf{q}, t)$ be number of rouleaux containing k red blood cells which have centre of mass between $\mathbf{x}$ and $\mathbf{x}+d\mathbf{x}$ and an end-to-end vector between $\mathbf{q}$ and $\mathbf{q}+d\mathbf{q}$ at time t.
Based on some ideas from the classical theory of network models for viscoelastic fluids we assume that erythrocytes at any point are contained in aggregates of different sizes, which continuously break up and aggregate with other aggregates. The rate of coalescing and breaking up depends on time, strain, shear rate and stress. The aggregates represented as dumbbells are transported, stretched and oriented in a flow. Key assumption of Owens' model is, that under condition of sufficiently low shear rates we use a linear spring flow for modelling of the dumbbells.
The continuity equation for ψ_k under condition of a homogeneous flow now reads:

$$\frac{\partial\psi_k}{\partial t} = -\frac{\partial}{\partial\mathbf{q}} \cdot \left(\nabla\mathbf{v} \cdot \mathbf{q}\psi_k - \frac{2k_BT}{\zeta_k}\frac{\partial\psi_k}{\partial\mathbf{q}} - \frac{2\mathbf{q}H}{\zeta_k}\psi_k\right) + h_k(\dot{\gamma}, t)\psi_{k,0} - g_k(\dot{\gamma}, t)\psi_k, \tag{2.36}$$

where h_k and g_k are rates of creation and destruction because of agglomeration and disaggregation of aggregates, respectively, k_B is Boltzmann's constant, T is the absolute temperature, H the Hookean spring constant and ζ_k drag coefficient dependent on the number of erythrocytes in an aggregate k.
We multiply equation (2.36) by $\mathbf{qq}$, we integrate over $\mathbf{q}$, integrate by parts, to obtain an evolution equation for the configuration tensor $< \mathbf{qq} >_{\psi_k}$:

$$< \overset{\triangledown}{\boldsymbol{qq}} >_{\psi_k} = \frac{4k_BT}{\zeta_k}kN_kI - \frac{4H}{\zeta_k} < \mathbf{qq} >_{\psi_k} + h_k < \mathbf{qq} >_{\psi_{k0}} - g_k < \mathbf{qq} >_{\psi_k}, \tag{2.37}$$

where an ensemble average is defined as

$$< . >_{\psi_k} = \int_{\mathbf{q}} .\psi_k(\mathbf{q}, t)d\mathbf{q}. \tag{2.38}$$

In equilibrium the following holds:

$$< \mathbf{qq} >_{\psi_{k0}} = \frac{k_BT}{H}kN_{k0}I, \tag{2.39}$$

due to the fact $g_k = h_k$ in equilibrium. We can than write the Kramers expression for the elastic extra-stress $\boldsymbol{\tau}_k$ originating from $N_k k$-mers in the following manner:

$$\boldsymbol{\tau}_k = H < \mathbf{qq} >_{\psi_k} - kN_kk_BTI. \tag{2.40}$$

If we substitute for $< \mathbf{qq} >_{\psi_k}$ from (2.40) into (2.37) we obtain

$$\begin{aligned}
&\frac{1}{H}(\boldsymbol{\tau}_k + k \overset{\triangledown}{N_k}\, k_B T I) \\
&= \frac{4k_B T}{\zeta_k} k N_k I - \frac{4}{\zeta_k}\left(\boldsymbol{\tau}_k + k N_k k_B T I\right) \\
&+ h_k k N_{k0} \frac{k_B T}{H} I - \frac{g_k}{H}\left(\boldsymbol{\tau}_k + k N_k k_B T I\right).
\end{aligned}$$

It holds that

$$k \overset{\triangledown}{N_k}\, k_B T I = k \frac{dN_k}{dt} k_B T I - k N_k k_B T \mathbf{D} \tag{2.41}$$

and

$$\frac{dN_k}{dt} = h_k N_{k0} - g_k N_k. \tag{2.42}$$

We will end with a new constitutive equation for $\boldsymbol{\tau}_k$:

$$\boldsymbol{\tau}_k + \left(\frac{4H}{\zeta_k} + g_k\right)^{-1} \overset{\triangledown}{\boldsymbol{\tau}_k} = k N_k k_B T \left(\frac{4H}{\zeta_k} + g_k\right)^{-1} \boldsymbol{D} \qquad k = 1, 2, 3, \ldots, \tag{2.43}$$

We can see, that the relaxation time

$$\mu_k = \left(\frac{4H}{\zeta_k} + g_k\right)^{-1} \tag{2.44}$$

contains not only the well known part from Oldroyd-B like model $\frac{\zeta_k}{4H}$, which causes, that the relaxation time μ_k is smaller than the mentioned relaxation time originating from Oldroyd-B model.

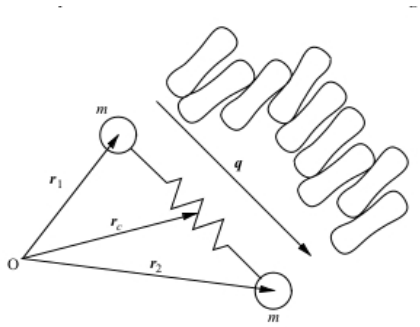

Figure 3: Rouleaux as an elastic dumbbell. From [10]

Owens derived following form of constitutive equation for elastic part of stress tensor due to k-mer

$$\boldsymbol{\tau}_k + \mu_k \left(\frac{\partial \boldsymbol{\tau}_k}{\partial t} + (\mathbf{u}\cdot\nabla)\boldsymbol{\tau}_k - \nabla\mathbf{u}\cdot\boldsymbol{\tau}_k - \boldsymbol{\tau}_k\cdot\nabla\mathbf{u}^T\right) = 2\eta_{pk}\dot{\boldsymbol{\gamma}}(\mathbf{u}), \tag{2.45}$$

where the symbol μ_k is the relaxation time of k-mer,

$$\eta_{pk} := k N_k k_B T \mu_k \tag{2.46}$$

is polymeric viscosity due to the k-mer. Here N_k is density of k-mers, therefore kN_k gives density density of 'mers' , i.e. red blood cells, taking part in k-mer. k_B is the Boltzmann constant, T temperature.
As the rouleaux are associating and disaggregating the relaxation time is not only function of shear rate, but it also depends on aggregate size.
Owens proceeds with the following simplification - the constitutive equation is summed up from $k = 1$ to $k = \infty$ to get

$$\boldsymbol{\tau} + \mu \left(\frac{\partial \boldsymbol{\tau}}{\partial t} + (\mathbf{u}\cdot\nabla)\boldsymbol{\tau} - \nabla\mathbf{u}\cdot\boldsymbol{\tau} - \boldsymbol{\tau}\cdot\nabla\mathbf{u}^T\right) = 2\eta_p\dot{\boldsymbol{\gamma}}(\mathbf{u}). \tag{2.47}$$

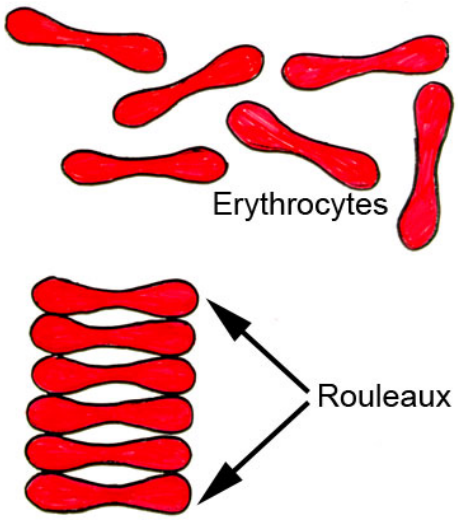

Figure 4: Rouleaux formation

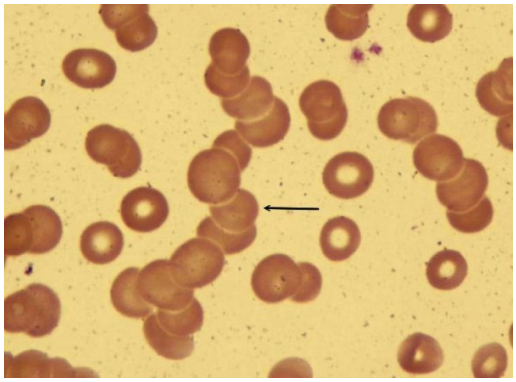

Figure 5: Rouleaux formation. From http://www.mediscuss.org/erythrocyte-sedimentation-rate-77.html

The key step in this procedure is substitution of the relaxation time μ_k with averaged relaxation time $\mu_{\hat{N}}$
Owens derived following equation for the time development of the average rouleaux size $\hat{N}$:

$$\frac{D\hat{N}}{Dt} + \frac{1}{2}b(\dot{\gamma})(\hat{N} - \hat{N}_{st})(\hat{N} + \hat{N}_{st} - 1) = 0, \tag{2.48}$$

where $b(\dot{\gamma})$ is a fragmentation rate and $\hat{N}_{st} = \hat{N}_{st}(\dot{\gamma})$ is the value of $\hat{N}$ in a steady simple shear flow with shear-rate $\dot{\gamma}$.
Owens supplied an equation for relaxation time μ:

$$\mu = \mu(\hat{N}, \dot{\gamma}) = \frac{\lambda_H \hat{N}}{1 + g_{\hat{N}}\hat{N}\lambda_H}, \tag{2.49}$$

where $g_{\hat{N}}$ is an aggregation coefficient of rouleaux of $\hat{N}$ cells:

$$g_{\hat{N}}\hat{N} = \frac{1}{2}b(\dot{\gamma})\hat{N}(\hat{N} - 1) + a(\dot{\gamma}). \tag{2.50}$$

In the equation $a(\dot{\gamma})$ is an aggregation rate for the RBC's and λ_H is the relaxation time of a single blood cell. Owens included in the model the Cross model viscosity:

$$\eta(\dot{\gamma})_p = \eta_0 \left(\frac{1 + \theta\dot{\gamma}^m}{1 + \beta\dot{\gamma}^m} \right). \tag{2.51}$$

To sum up, Owens solved the following system of equations:

$$\begin{gathered} Re\frac{D\mathbf{u}}{Dt} - 2\eta_s \nabla \cdot \mathbf{D} - \nabla \cdot \boldsymbol{\tau} + \nabla p = 0, \\ \nabla \cdot \mathbf{u} = 0, \\ \frac{D\hat{N}}{Dt} + \frac{1}{2}b(\dot{\gamma})(\hat{N} - \hat{N}_{st})(\hat{N} + \hat{N}_{st} - 1) = 0, \\ \boldsymbol{\tau} + De(\dot{\gamma}, \hat{N})\left(\frac{\partial \boldsymbol{\tau}}{\partial t} + (\mathbf{u} \cdot \nabla)\boldsymbol{\tau} - \nabla\mathbf{u} \cdot \boldsymbol{\tau} - \boldsymbol{\tau} \cdot \nabla\mathbf{u}^T \right) = De(\dot{\gamma}, \hat{N})\boldsymbol{D}, \end{gathered} \tag{2.52}$$

where due to non-dimensionalisation the Deborah number is given by

$$De = \mu\frac{U}{L}, \tag{2.53}$$

with U, L being characteristic velocity and length, respectively.

2.2.3 Shear induced migration and it's modeling

In the following we will be mainly dealing with flows of concentrated suspensions. We know from experiments, that there is a shear-induced migration of particles. This behaviour was observed in several experimental configurations. The phenomenon was firstly studied in [22]. The discovery of the new phenomenon initiated new development of rheology. We can divide corresponding mathematical models into two branches.
The first one, which we will follow, gives an expression for the particle migration flux $\boldsymbol{j}_\perp \approx \nabla \cdot \boldsymbol{\Sigma}_p$. $\boldsymbol{\Sigma_p}$ is the particle contribution to the bulk stress.
The second one, called in [21] phenomenological, develops the particle migration flux of the form $\boldsymbol{j}_\perp \approx -\nabla\dot{\gamma}$, where $\dot{\gamma}$ is the shear rate. It is the approach of the seminal work [22].
In the introduction of [21] is discussed applicability of the phenomenological model. There and in the references therein is shown, that the phenomenological model does not capture some experimental configurations appropriately.
On the other hand the first approach, called suspension rheology approach, is, according to [21], successful in the description of wider set of experimental data than the phenomenological model is.
The main added value of suspension rheology model is incorporation of normal stresses. In [21] is shown, that the introduction of particle-fraction dependent and anisotropic suspension normal stresses captures relatively well observed particle migration in curvilinear flows of monodisperse suspensions.

We will now derive the expression for the flux $\boldsymbol{j}_\perp$ in a vein similar to [21] and [18]. It is supposed, of course that, the particle phase can be approximated as a continuum. If we suppose low Reynolds number the following equations for mass and momentum balances for suspension can be derived:

$$\nabla \cdot \mathbf{u} = 0, \tag{2.54}$$

$$\nabla \cdot \Sigma + < \rho > \mathbf{g} = 0, \tag{2.55}$$

where $< \rho >$ is the mixture density, $\mathbf{u}$ is the bulk suspension velocity, Σ is the bulk suspension stress, $< \rho > \mathbf{g}$ is the mean gravity force. We can write particle-phase mass balance as

$$\frac{\partial \Phi}{\partial t} + \mathbf{u} \cdot \nabla \Phi = -\nabla \cdot \mathbf{j}_\perp, \tag{2.56}$$

where $\mathbf{j}_\perp = \Phi(\mathbf{u}_p - \mathbf{u})$ is the particle migration flux relative to the bulk motion, $\mathbf{u}_p$ is the particle phase average velocity, Φ is the particle volume fraction.
In [18] the migration flux is obtained from the particle momentum balance:

$$0 = \nabla \cdot \boldsymbol{\Sigma}_P + n < \mathbf{F}^H > + \Phi \Delta\rho \mathbf{g}, \tag{2.57}$$

where n is the number density of particles, $\Delta\rho = \rho_p - \rho_f$ is the excess density of particles and $\boldsymbol{\Sigma}_P$ the particle contribution to the bulk stress.
The mean drag force on any particle $< \mathbf{F}^H >$ may be derived for Stokes flow:

$$< \mathbf{F}^H > = -6\pi\eta_0 a f^{-1}(\Phi)(\mathbf{u}_p - \mathbf{u}), \tag{2.58}$$

where $f(\Phi)$ represents the mean mobility of the particle phase, i.e. f^{-1} is the mean resistance, η_0 is the viscosity of the suspending fluid. If we substitute (2.58) into (2.57) we obtain, under supposition of neutrally buoyant particles, the following expression for the particle migration flux:

$$\mathbf{j}_\perp = \Phi(\mathbf{u}_p - \mathbf{u}) = \frac{2a^2}{9\eta_0} f(\Phi) \nabla \cdot \boldsymbol{\Sigma}_P. \tag{2.59}$$

Therefore the final version of the flux is

$$J = \frac{2}{9} a^2 \frac{f(\Phi)}{\eta_0} \nabla \cdot \boldsymbol{\Sigma_p}. \tag{2.60}$$

We will show the derivation of the constitutive equation for $\boldsymbol{\Sigma} = \boldsymbol{\Sigma}_f + \boldsymbol{\Sigma}_p$ for the bulk suspension stress. In [21] the fluid stress is assumed to be

$$\boldsymbol{\Sigma}_f = - < P >_f \boldsymbol{I} + 2\eta_0 \boldsymbol{D}, \tag{2.61}$$

where $< P >_f$ is the fluid phase averaged pressure, $\boldsymbol{I}$ is identity tensor,$\boldsymbol{D}$ local rate of strain tensor. For definition of the averages and the averaging procedure see [21] and references therein.
The particle stress proposed in [21] has the following form

$$\boldsymbol{\Sigma}_p = -\eta_0\eta_n(\Phi)\dot{\gamma}\boldsymbol{Q} + 2\eta_0\eta_p(\Phi)\boldsymbol{D}, \tag{2.62}$$

where η_p is a monotonous function of particle volume fraction Φ, $\boldsymbol{Q}$ is the tensor parameter of anisotropy to be specified later. In [21] such a simple form of particle stress tensor was chosen in order to get some analytical steady state predictions. However it is still rich enough to capture the normal stresses, which enable the description of the particle migration phenomenon, as was stated above. It is done so via introduction of "normal stress viscosity" $\eta_n(\Phi)$, whose form is given in [21] as

$$\eta_n(\Phi) = K_m \frac{(\Phi/\Phi_m)^2}{(1-\Phi/\Phi_m)^2}, \tag{2.63}$$

where Φ_m is the maximum packing density, K_m is a constant determined by the fit to experiment.

2.2.4 Modified Owens' model

We know from measurements, that red blood cells tend populate the central area of a vessel. Because of that effect they leave a cell depleted region near the vessel walls.
The behaviour is interesting for us not only because it explains Fahraeus and Fahraeus-Lindquist effect. There is an another reason - red blood cells expell by their inward migration other blood species from the central regions of a vessel. This effect is very important for the blood coagulation process as the key factors of blood coagulation such as blood platelets and chemical species are present in elevated concetrations near the vessel wall. In the case of a vessel injury, these elements of blood are near the site of the damaged vessel wall.
[17] added to the equations of conservation (continuity and momentum) a transport equation for the hematocrit. It was supposed the following general form

$$\frac{D\Phi}{Dt} = -\nabla \cdot \mathbf{J}. \tag{2.64}$$

In [18] it is derived an equation for the particle flux $\mathbf{J}$, see (2.60), supposing that the particles, in our case red blood cells, have the spherical shape.

However, if we want to develop a blood model, where we want to take into account the fact, that red blood cells can create aglomerates, rouleaux, we must modify the functinal form for mobility $f(\Phi)$.
Up to know the mobility increased as the concentration, in this case hematocrit, decreased. We will now take the mobility as a function of both Φ and $\hat{N}$, in the case of blood, of the hematocrit and the average rouleaux size, respectively. It is natural to suppose that the mobility increases as the rouleaux fragment. Therefore the largest mobility should have solitary red blood cells, which correspond to the value $\hat{N}$ equal to 1. From now on we will take the mobility as a function of both Φ and $\hat{N}$, i.e. $f(\Phi, \hat{N})$.
We will now delve into the constitutive equations. As in [17] we will decompose the Cauchy stress of the bulk into two parts, that of solvent and that of particle phase:

$$\boldsymbol{\Sigma} = \boldsymbol{\Sigma_f} + \boldsymbol{\Sigma_p}. \tag{2.65}$$

We will suppose that the solvent part behaves as a Newtonian fluid:

$$\boldsymbol{\Sigma_f} = -p\mathbf{I} + 2\eta_0\mathbf{D}, \tag{2.66}$$

where p is the solvent pressure and η_0 is the viscosity of the solvent.
In similar vein as in [17] we write down the constituive equation for the particle phase:

$$\boldsymbol{\Sigma_p} = \boldsymbol{\Sigma_p^{NS}} + \boldsymbol{\tau}, \tag{2.67}$$

where $\boldsymbol{\Sigma_p^{NS}}$ corresponds to the particle pressure, $\boldsymbol{\tau}$ is the elastic part of extra stress tensor, i.e. the contribution to the extra stress from the particle(red blood cells) phase.
In [17] was supposed that the particle pressure $\boldsymbol{\Sigma_p^{NS}}$ has the following functional form:

$$\boldsymbol{\Sigma_p^{NS}} = -\eta_0\alpha(\Phi)\dot{\gamma}\boldsymbol{Q}, \tag{2.68}$$

where $\alpha(\Phi)$ is growing function of the particle fraction, which could be taken as (2.63). Φ, $\boldsymbol{Q}$ is the tensor parameter of anisotropy:

$$\boldsymbol{Q} = \begin{pmatrix} 1 & 0 & 0 \\ 0 & \lambda_2 & 0 \\ 0 & 0 & \lambda_3 \end{pmatrix}, \tag{2.69}$$

where $\lambda_2 \approx 0.8$ and $\lambda_3 \approx 0.5$ are in good agreement with concentrated suspension rheology[add references].
Owens used the relation (2.51) in order to incorporate the shear-thinning behaviour of the blood into his model. We will suppose, that the viscosity is not only shear-rate dependent, but it depends on the hematocrit too. This fact was experimentally verified [19]. Therefore we propose the following form of the viscosity:

$$\eta_p(\dot{\gamma}, \Phi) = \eta_0 \left(\frac{1 + \theta \dot{\gamma}^m}{1 + \beta \dot{\gamma}^m} \right) h(\Phi), \tag{2.70}$$

where $h(\Phi)$ is increasing function of the hematocrit Φ. In [20] was proposed a functional form for dependence of blood viscosity on shear-rate, hematocrit and temperature. However we will restrict our attention on healthy humans, therefore we will not need the functional dependence of the blood viscosity on temperature.
It must be noted, that we can simplify our model by taking into account only hematocrit dependent part polymeric viscosity. Actually there is research on that topic originating from [19]. The polymeric viscosity would then look like

$$\eta_p(\Phi) = \eta_0 H(\Phi), \tag{2.71}$$

where $H(\Phi)$ is an appropriate function fitted to data. We have limited ourselves for our initial stage of modeling to shear-rate dependent viscosity. There is however a large field for extension of the model in the way of hematocrit dependent viscosity.
To sum up, in our modified model we solve the following set of equations:

$$\begin{gathered} Re \frac{D\mathbf{u}}{Dt} - \nabla \cdot \boldsymbol{\Sigma} = 0, \\ \nabla \cdot \mathbf{u} = 0, \\ \boldsymbol{\tau} + De(\dot{\gamma}, \hat{N}) \left(\frac{\partial \boldsymbol{\tau}}{\partial t} + (\mathbf{u} \cdot \nabla)\boldsymbol{\tau} - \nabla \mathbf{u} \cdot \boldsymbol{\tau} - \boldsymbol{\tau} \cdot \nabla \mathbf{u}^T \right) = 2De(\dot{\gamma}, \hat{N}) \boldsymbol{D}, \\ \frac{D\hat{N}}{Dt} + \frac{1}{2} b(\dot{\gamma})(\hat{N} - \hat{N}_{st})(\hat{N} + \hat{N}_{st} - 1) = 0, \\ \frac{D\Phi}{Dt} = -\nabla \cdot \boldsymbol{J}, \end{gathered} \tag{2.72, 2.73}$$

where

$$\mathbf{J} = \frac{2}{9} a^2 \frac{f(\phi)}{\eta_0} \nabla \cdot \boldsymbol{\Sigma_p}$$

and

$$\boldsymbol{\Sigma} = \boldsymbol{\Sigma_f} + \boldsymbol{\Sigma_p} = -pI + 2\eta_0 \boldsymbol{D} + \boldsymbol{\Sigma_p^{NS}} + \boldsymbol{\tau}$$

3 Numerical methods

We concentrate in this work on mathematical modelling of blood flow. Hence we should describe the numerical treatment of viscoelastic models of fluids. The majority of methods is described in [11].

3.1 DEVSS

In order to increase convergence in viscoelastic flow simulations one can increase coercivity of the elliptic operator in the momentum equation. An auxiliary variable $\boldsymbol{d}$ is added to the system of equation to retain consistency of it.(See (3.4))

3.2 SUPG

Convection dominated problems require special numerical treatment as their Galerkin formulation suffers from spurious oscillations not present in their true solution.
The first possibility is to introduce into the system artificial diffusion in all direction. It can however lead to the blurring of sharp layers and nonphysical increase of the concentration in some regions.
The SUPG approach which is more physically accurate was therefore proposed. Its crux lies in the introduction of artificial diffusion in streamline upwind direction.
Mathematically, the introduction of artificial diffusion can be formulated as a modification of the test function of the convective term. On this basis is developed the SUPG stabilization method for finite element method, but for consistency, the modified test function is applied to all terms of the weak form. In that case, the exact solution of the problem satisfies the weak form.
In our case, the test function ϕ_τ is modified in the following manner:

$$\phi_\tau \to \phi_\tau + \alpha_h^{SU} \mathbf{u} \cdot \nabla \phi_\tau, \tag{3.1}$$

where α_h^{SU} is a stabilisation parameter.
The test function for $\hat{N}$ is modified accordingly:

$$\phi_{\hat{N}} \to \phi_{\hat{N}} + \alpha_h^{SU} \mathbf{u} \cdot \nabla \phi_{\hat{N}}. \tag{3.2}$$

The test function for $\hat{\Phi}$ is modified in similar vein:

$$\phi_\Phi \to \phi_\Phi + \alpha_h^{SU} \mathbf{u} \cdot \nabla \phi_\Phi. \tag{3.3}$$

We will not write the modified test function in the system of equations for simplicity. We will implicity treat them as modified in the described manner.

3.3 Time discretization

For the time discretization of the system we use implicit Euler scheme, which is first-order scheme and unconditionally stable.
We divided the computation time interval I into n time steps $< t^k, t^{k+1} >$, for $k = 0, \dots n-1$, where $t^0 = 0$ and $t^n = T$. The step length of interval $< t^k, t^{k+1} >$ is $\Delta t^k = t^{k+1} - t^k$. We take an equidistant partition of time period, therefore the step length is constant Δt.

3.4 Discretization in space

We discreitze the system of equation in space by standard finite element method. Starting from a weak form using test functions from appropriate spaces, these spaces are then discretized to finite dimensional spaces which transforms our system of partial differential equations to the set of algebraic equations.
The approximation spaces are

$$\mathcal{U}_h = \left\{ \mathbf{u}_h \in C_0(\Omega) : \mathbf{u}_h|_K \in Q_2^d, \forall K \in M_h \right\},$$

$$\mathcal{P}_h = \left\{ p_h \in C_0(\Omega) : p_h|_K \in Q_1, \forall K \in M_h \right\},$$

$$\mathcal{N}_h = \left\{ \hat{N}_h \in C_0(\Omega) : \hat{N}_h|_K \in Q_1, \forall K \in M_h \right\},$$

$$\mathcal{T}_h = \left\{ \boldsymbol{\tau}_h \in C_0(\Omega) : \boldsymbol{\tau}_h|_K \in Q_1^{3\times 3, sym}, \forall K \in M_h \right\},$$

$$\mathcal{D}_h = \mathcal{T}_h,$$

$$\mathcal{J}_h = \left\{ \hat{N}_h \in C_0(\Omega) : \hat{N}_h|_K \in Q_1, \forall K \in M_h \right\}.$$

The discrete form of equations is following:

$$Re\left\langle \frac{(\mathbf{u}_h^n - \mathbf{u}_h^{n-1})}{\Delta t}, \phi_{\mathbf{u}} \right\rangle + Re\left\langle (\mathbf{u}_h^n \cdot \nabla)\mathbf{u}_h^n, \phi_{\mathbf{u}} \right\rangle + (\alpha + 2\eta_s)\left\langle \boldsymbol{D}_h^n, \nabla\phi_{\mathbf{u}} \right\rangle \tag{3.4}$$

$$= \left\langle \nabla \cdot \boldsymbol{\tau}_{\boldsymbol{h}}^{\boldsymbol{n}}, \phi_{\mathbf{u}} \right\rangle + \alpha\left\langle \mathbf{d}_h^n, \nabla\phi_{\mathbf{u}} \right\rangle \qquad \forall\phi_{\mathbf{u}} \in \mathcal{U}_{test,h}, \tag{3.5}$$

$$\langle \nabla \cdot \mathbf{u}_h^n, \phi_p \rangle = 0 \qquad \forall\phi_p \in \mathcal{P}_{test,h},$$

$$\langle \mathbf{d}_h^n, \phi_{\mathbf{d}} \rangle = \langle \mathbf{D}_h^n, \phi_{\mathbf{d}} \rangle \qquad \forall\phi_{\mathbf{d}} \in \mathcal{D}_{test,h}, \tag{3.6}$$

$$\left\langle \frac{\hat{N}_h^n - \hat{N}_h^{n-1}}{\Delta t}, \phi_{\hat{N}} \right\rangle + \left\langle (\mathbf{u}_h^n \cdot \nabla)\hat{N}_h^n, \phi_{\hat{N}} \right\rangle + \left\langle \frac{1}{2}b(\dot{\gamma}^n)(\hat{N}_h^n + \hat{N}_{st}(\dot{\gamma}^n) - 1)\hat{N}_h^n, \phi_{\hat{N}} \right\rangle$$

$$= \left\langle \frac{1}{2}b(\dot{\gamma}^n)(\hat{N}_h^n + \hat{N}_{st}(\dot{\gamma}^n) - 1)\hat{N}_{st}(\dot{\gamma}^n), \phi_{\hat{N}} \right\rangle \qquad \forall\phi_{\hat{N}} \in \mathcal{N}_{test,h},$$

$$\langle \boldsymbol{\tau}_h^n, \phi_{\boldsymbol{\tau}} \rangle + \left\langle De(\hat{N}_h^n)\left(\frac{\boldsymbol{\tau}_h^n - \boldsymbol{\tau}_h^n}{\Delta t} + (\mathbf{u}_h^n \cdot \nabla)\boldsymbol{\tau}_h^n - \nabla\mathbf{u}_h^n \cdot \boldsymbol{\tau}_h^n - \boldsymbol{\tau}_h^n \cdot \nabla\mathbf{u}_h^n \right), \phi_{\boldsymbol{\tau}} \right\rangle$$

$$= \langle De\mathbf{D}_h^n, \phi_{\boldsymbol{\tau}} \rangle \qquad \forall\phi_{\boldsymbol{\tau}} \in \mathcal{T}_{test,h},$$

$$\left\langle \frac{\Phi_h^n - \Phi_h^{n-1}}{\Delta t}, \phi_\Phi \right\rangle + \langle (\mathbf{u}_h^n \cdot \nabla)\Phi_h^n, \phi_\Phi \rangle = -\langle \mathbf{J}_h^n, \phi_\Phi \rangle \qquad \forall\phi_\Phi \in \mathcal{J}_{test,h}. \tag{3.7}$$

3.5 Experimental setting

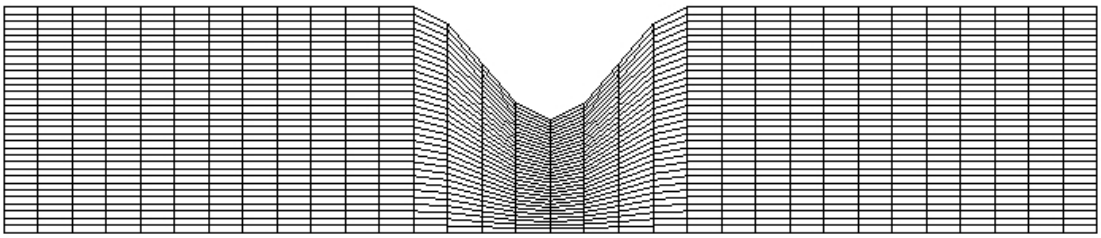

Figure 6: Mesh for stenosis

4 Results

4.1 Stenosis

We have imposed parabolic boundary condition for velocity on the inlet of the channel. We have supposed zero boundary condition for stress, nontrivial boundary conditions for average rouleaux size on inlet and physiological value of hematocrit on inlet.

We can see in the Figure 7, that behind the stenosis there is a stagnation point area. From the series of development snapshots (we are computing in non-dimensinal time) Figure 8 we can see, that there are high values of average rouleaux size outwards of stream. The high values are at the position of stagnation flow, as we expected. Namely in stagnation point there are low values of shear rates and our model was based on supposition, that buildup of rouleaux occurs mainly under low shear rate conditions.
We have developed a numerical method to solve the extended Owens' model. However we still need further testing of suitable stabilizations for fully physical setting to increase the robustness of the numerical solver.

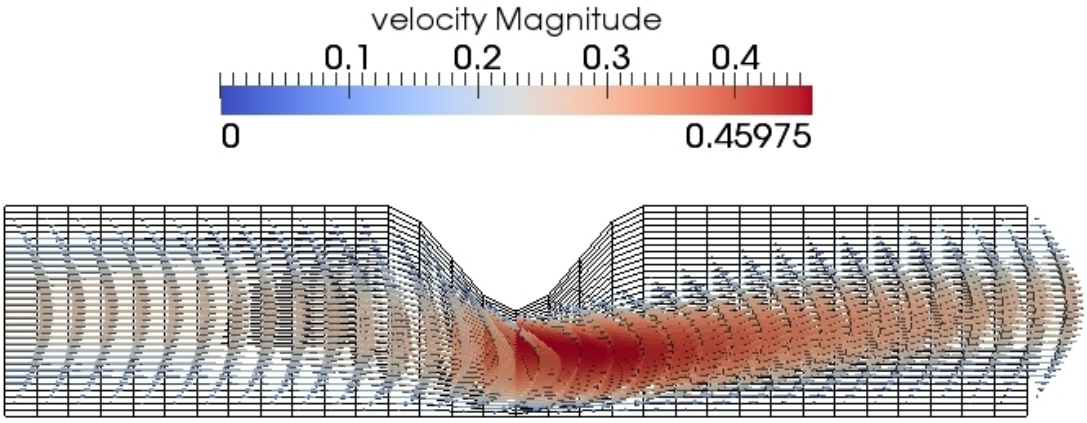

Figure 7: Velocity field for stenosis

5 Conclusions

We developed a non-newtonian model of blood capturing the erythrocytes separation phenomenon. Our model is based on Owens' model of blood[8], which falls into microstructure based models. We have preferd such a kind of model, because it treats the thixotropy of blood.
Our modification of Owens' model of blood lies in the introduction of an advected field for the volume fraction of erythrocytes into the system of equations. We have followed the proposals given in [17], wherein it is proposed to treat blood as suspension of erythrocytes in blood plasma. We have taken the erythrocytes as rigid spheres with drag exerted on them derived under the assumption of Stokes flow. Such a kind of simplification could seem very rough, but we can not do much more if we want to be able to compute problems on realistic geometries. We have chosen a sample geometry - a channel with stenosis. We arrived at interesting results

6 Acknowledgments

The study was supported by the Charles University in Prague, project GA UK No.694912

This work was supported by the IT4Innovations Centre of Excellence project (CZ.1.05/1.1.00/02.0070), funded by the European Regional Development Fund and the national budget of the Czech Republic via the Research and Development for Innovations Operational Programme, as well as Czech Ministry of Education, Youth and Sports via the project Large Research, Development and Innovations Infrastructures (LM2011033).

References

[1] Thurston, G., Viscoelasticity of human blood, Biophysical Journal, 1972

[2] Aarts, P., van den Broek, S. A., Prins, G., Kuiken, G., Sixma, J., and Heethaar, R. (1988). Blood platelets are concentrated near the wall,Arterioscler Thromb Vasc Biol

[3] Hathcock, J., Flow effects on coagulation and thrombosis. Arteriosclerosis thrombosis and vascular biology, 26(8):17291737,2006

[4] Colman, R. W,Hemostasis and Thrombosis: Basic Principles and Clinical Practice, Lippincott Williams Wilkins,2006

[5] K.R. Rajagopal and A.R. Srinivasa, A thermodynamic frame work for rate type fluid models, J. Non-Newtonian Fluid Mechanics 88,2000

$t = 0$

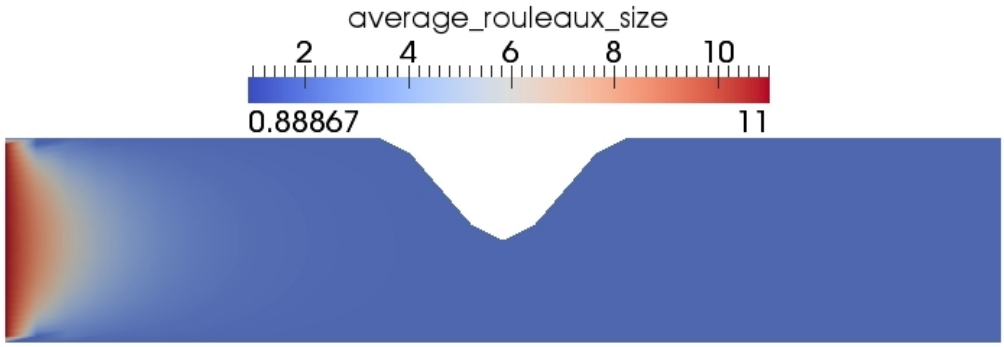

$t = 100$

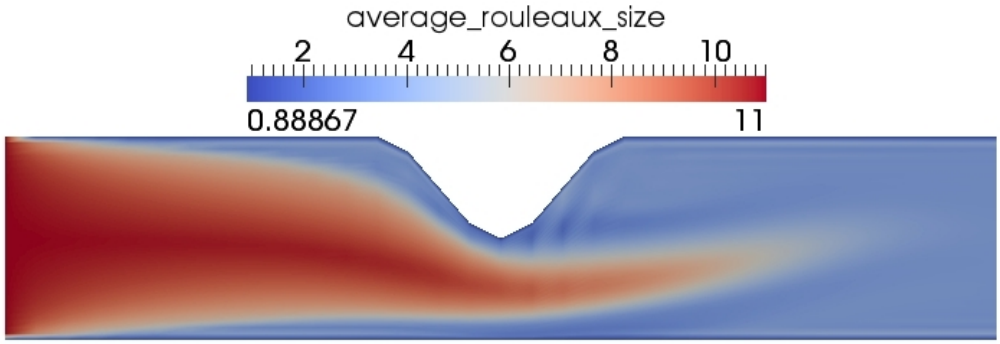

$t = 1000$

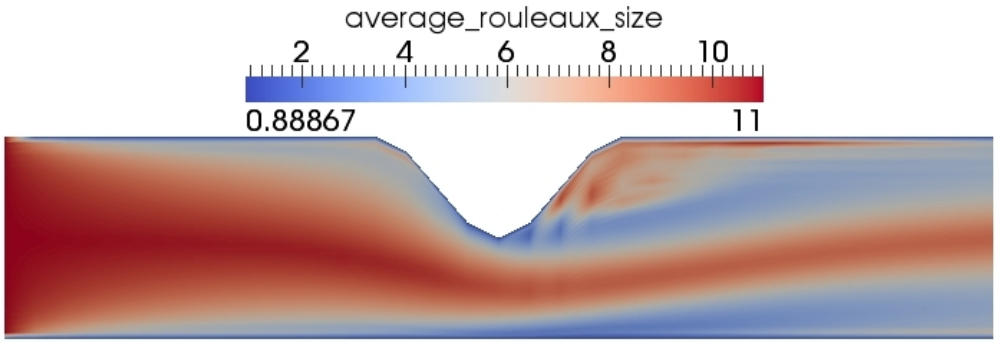

Figure 8: Average rouleaux size distribution at several time steps

[6] K.R. Rajagopal and A.R. Srinivasa, On the thermodynamics of materials that have multiple natural configurations Part I: Viscoelasticity and classical plasticity, ZAMP 55,2004

[7] K.R. Rajagopal and A.R. Srinivasa, On thermomechanical restrictions of continua, Proceedings of the Royal Society 460 ,2004

[8] R. G. Owens, A new microstructure-based constitutive model for human blood. J.Non-Newtonian Fluid Mech., 140 (2006) 57-70

[9] Fang, J.F., Owens, R.G. (2006) Numerical simulations of pulsatile blood flow using a new constitutive model, Biorheology. 2006;43(5):637-60.

[10] Iolov A., Kane A.S., Bourgault Y., Owens R.G., Fortin A. (2011)A finite element method for a microstructure-based model of blood, International Journal for Numerical Methods in Biomedical Engineering Volume 27, Issue 9, pages 13211349, September 2011

[11] R. G. Owens, T.N. Phillips, Computational rheology, Imperial College press, 2005

[12] T. Bodnar, A. Sequeira,Numerical Simulation of the Coagulation Dynamics of Blood,Computational and Mathematical Methods in Medicine Volume 9 (2008), Issue 2, Pages 83-104

[13] L. Pirkl,T. Bodnar, The blood flow simulations using generalized Newtonian models,Colloquium FLUID DYNAMICS 2007 Institute of Thermomechanics AS CR, Prague. October 24 - 26, 2007

[14] M. Anand,Modelling the growth and dissolution of clots in flowing blood, PhD thesis, Texas A&M University

[15] M. Anand, J.Kwack, A. Masud,A new generalized Oldroyd-B model for blood flow in complex geometries, International Journal of Engineering Science Volume 72, November 2013, Pages 7888

[16] L.M. Crowl, A. L. Fogelson, Computational model of whole blood exhibiting lateral platelet motion induced by red blood cells, Int. j. numer. method. biomed. eng. 2010 March 1; 26(3-4): 471487

[17] Tokarev, A., Panasenko, G., and Ataullakhanov, F., Segregation of Flowing Blood: Mathematical Description, Mathematical Modelling of Natural Phenomena 6.5 (2011): 281-319. ¡http://eudml.org/doc/222413¿.

[18] R. Miller, J. Morris,Normal stress-driven migration and axial development in pressure-driven flow of concentrated suspensions,ournal of Non-Newtonian Fluid Mechanics, Vol. 135, No. 2-3. (30 May 2006), pp. 149-165

[19] Roe E. Wells, Edward W. Merrill,Influence of flow properties of blood upon viscosity-hematocrit relationships,J Clin Invest. 1962 August; 41(8): 15911598.

[20] Eckmann DM, Bowers S, Stecker M, Cheung AT., Hematocrit, volume expander, temperature, and shear rate effects on blood viscosity.,Anesth Analg. 2000 Sep;91(3):539-45. December 2010

[21] Morris, J. F. ,Boulay, F. Curvilinear flows of non colloidal suspensions: The role of normal stresses

[22] Leighton, D.,Acrivos, A., The shear-induced migration of particles in concentrated suspensions Journal of Fluid Mechanics / Volume 181 / September 1987, pp 415-439

[23] Deville, M.O., Gatski, T.B, Mathematical modeling for complex fluid and flows, Springer 2012